Off-Grid Compressed Sensing for GMTI using SAR Images

Ludger Prünte
Fraunhofer Institute for High Frequency Physics and Radar Techniques FHR
Fraunhofer Str. 20
53343 Wachtberg, Germany
Email: ludger.pruente@fhr.fraunhofer.de

***Abstract*—The choice of the grid for generating the sparsity inducing basis or rather a corresponding dictionary is a central point of compressed sensing and sparse approximation. A poorly chosen grid corrupts the reconstruction performance. Here we consider the problem of ground moving target indication from several – already processed – synthetic aperture radar images and apply a recently introduced method for reducing the effect of the grid.**

I. Introduction

The basis or rather dictionary $\mathbf{\Psi}$ defining a sparse representation $\mathbf{x}$ for compressed sensing (CS) or sparse approximation is usually generated using an equidistant grid $\mathcal{G}$. A wide grid spacing results directly in signals that are not represented by the grid. These are reconstructed consequently by approximation with a superposition of signals represented by several neighboring gridpoints (i.e. neighboring entries in $\mathbf{x}$), resulting in less sparse representations. On the other hand a fine grid reduces the performance of CS algorithms (see Section II). Several approaches to mitigate the grid-effect are proposed in literature, e.g. by definition of a minimal distance between two nonzero entries of $\mathbf{x}$ as in [1] or by adaptively modifying $\mathbf{\Psi}$ (see [2]). Here we use the variant introduced in [3], that computes for every entry of $\mathbf{x}$ an additional coefficient, representing the distance from the gridpoint. This gives the opportunity to decrease the grid size (compared to standard CS) and improve the performance of CS due to lower mutual coherence and computation time.

In this paper we apply this approach to the problem of ground moving target indication (GMTI) on the basis of different synthetic aperture radar (SAR) images. This problem has been established since the introduction of along-track interferometry (ATI) and displaced phase center analysis (DPCA). While the two mentioned methods allow just two receiving antenna channels, more sophisticated methods – like the EDPCA (cf. [4]) – also permit the usage of a higher number of channels.

In [5] a first SAR-GMTI method based on CS was presented. Here $\mathcal{G}$ is a grid

$$\mathcal{G}_v = v_0 + \delta_v \cdot \{0, \ldots, N-1\}$$

of velocities. Since the velocity of a target is not known in advance, an a priori adaption of the grid is impossible and velocities v with not neglibible distance to $\mathcal{G}_v$ occur regularly, decreasing the performance of CS.

II. Compressed Sensing and Grid Effects

Let $\mathbf{y} = \mathbf{A}\mathbf{x} + \mathbf{n} \in \mathbb{C}^M$ be a vector of noisy measurements of a $\mathcal{G}_v$-discretized sparse scenery $\mathbf{x} \in \mathbb{C}^N$.

$$\mathbf{A} = [\mathbf{a}(v_0), \ldots, \mathbf{a}(v_0 + (N-1)\delta_v)] \in \mathbb{C}^{M \times N}$$

represents the likewise discretized measurement process, realized by the product $\mathbf{A} = \mathbf{\Phi}\mathbf{\Psi}$ of sparsifying matrix $\mathbf{\Psi}$ and the actual measurement process $\mathbf{\Phi}$. Here $\mathbf{a} : \mathbb{R} \mapsto \mathbb{C}^M$ represents a differentiable function, mapping the across-track velocities of the gridpoints to the space of measurements. The aim is (cf. [6]) to reconstruct a sparse $\mathbf{x}$ via a minimization like

$$\hat{\mathbf{x}} = \underset{\mathbf{x}}{\operatorname{argmin}} \|\mathbf{A}\mathbf{x} - \mathbf{y}\|_2 \text{ such that } \|\mathbf{x}\|_0 < \tau', \tag{1}$$

where the ℓ_0-norm is mathematically intractable, but enforces the sparsity of $\mathbf{x}$. Here we consider convex relaxation (also known as BP or LASSO) for solving this problem, so replacing $\|\cdot\|_0$ by $\|\cdot\|_1$ and τ' by τ, resulting in

$$\hat{\mathbf{x}} = \underset{\mathbf{x}}{\operatorname{argmin}} \|\mathbf{A}\mathbf{x} - \mathbf{y}\|_2 \text{ such that } \|\mathbf{x}\|_1 < \tau. \tag{2}$$

The quality of this relaxation depends (cf. [6]) on the mutual coherence

$$\mu(\mathbf{A}) \propto \max_{k \neq l} \langle \mathbf{a}(v_k), \mathbf{a}(v_l) \rangle.$$

Since $\mathbf{a}$ is a continuous function, $\mu(\mathbf{A})$ is especially large for directly neighboring gridpoints, so $v_k - v_l = \delta_v$. Hence reconstruction is not possible, if δ_v is too small.

One approach to mitigate the effect of the grid spacing was introduced in [3]: $\mathbf{\Psi}$ and consequently $\mathbf{A}$ are amended by additional atoms, giving the opportunity to approximate all parameters of a signal

$$\mathbf{y} = \sum_i b_i \mathbf{a}(v_i) \text{ with } v_i \notin \mathcal{G}_v, \tag{3}$$

i.e. to estimate the distances of the v_i to the neighboring gridpoints in addition to estimating b_i. This is e.g. done by considering the Taylor expansion of first degree for a velocity v in the interval $[v_n - \delta_v/2, v_n + \delta_v/2]$, i.e.

$$b\mathbf{a}(v) \approx b\mathbf{a}(v_n) + b(v - v_n)\frac{\partial}{\partial v}\mathbf{a}(v). \tag{4}$$

Letting

$$\hat{\mathbf{A}} = \left[A, \frac{\partial A}{\partial v}\right] \in \mathbb{C}^{M \times 2N}$$

and reconstructing

$$\hat{\mathbf{x}} = [x_{0,0}, \ldots, x_{0,N}, x_{1,0}, \ldots, x_{1,N}]$$

analogous to (2), the coefficients $x_{0,n}$ and $x_{1,n}$ correspond to b and $b(v - v_n)$ in (4). Consequently, a signal like $\mathbf{y}$ in (3) can be reconstructed, if the sparsity assumption is fulfilled.

Since every target with an off-grid velocity is represented by just two nonzero coefficients, there is no necessity for a dense grid for sparse representation of targets, as long as the grid is dense enough to separate targets. Consequently δ_v may be enlarged, reducing $\mu(\hat{\mathbf{A}})$. Moreover, $\mathbf{a}(v_n)$ and $\frac{\partial}{\partial v}\mathbf{a}(v_n)$ are usually almost orthogonal to each other. Hence the coherence $\mu(\hat{\mathbf{A}})$ is of course larger or equal than $\mu(\mathbf{A})$ for the same δ_v, but usually smaller than the coherence of $\mathbf{A}$ for $\delta_V/2$, having the same number of columns.

Different expansions like a polar interpolation on a circle defined by $\mathbf{a}(v_n - \delta_v/2), \mathbf{a}(v_n)$ and $\mathbf{a}(v_n + \delta_v/2)$ are of interest as well

and more accurate, but enlarge the number of coefficients and enforce additional side conditions. See [3] for further theoretical considerations. Moreover, the combined computation of data having the same structure of nonzero elements using a multimeasurement vector approach (MMV, see [6]) is possible and will increase the reconstruction performance.

III. Velocity Estimation in SAR Images

For airborne multichannel stripmap synthetic aperture radar (SAR) pulses are transmitted from approximately equidistant positions on a linear flight path. The waves that are backscattered from earth are received via M antennas. Here these are arranged in direction of flight at positions $\mathbf{d} = [d_1, \ldots, d_M]$ and measure amplitude, phase and delay time. Every target is illuminated by several pulses. In consequence – after some preprocessing – a two-dimensional SAR image of size $K \times L$ may be computed from every channel via a classical matched filter approach. Here moving targets are shifted parallel to the flightpath by $\Delta x = R \cdot v / v_P$, where v_P is the platform's velocity, v the across-track component of the target's velocity and R is the distance (slant range) between them. In consequence superposition of objects of different across-track velocities are possible. Especially moving and non moving targets can be imaged to the same pixel of the SAR image, indepentently from the the pixel size.

Let $\mathbf{Y} \in \mathbb{C}^{K \times L \times M}$ be a stack of M SAR images from the different channels. For every pixel (k, l) there are M measurements $\mathbf{y}_{k,l} \in \mathbb{C}^M$, representing a superposition of targets of different velocities. Here a target of across-track velocity v_n generates a signal which is normalized to

$$\mathbf{a}(v_n) = \frac{1}{\sqrt{M}} \exp\left(\frac{2\pi j}{\lambda} \cdot \frac{v_n}{v_P} \cdot \mathbf{d}\right),$$

where λ denotes the wavelength and $v_n \in \mathcal{G}_v$. Defining $\mathbf{A}$ as in Section II, we obtain an excerpt of the Fourier matrix, a case well known in CS theory. Moreover, the expansion to the off-grid case $\hat{\mathbf{A}}$ is performed via the additional, normalized columns

$$\frac{\frac{\partial \mathbf{a}(v_n)}{\partial v}}{\left\| \frac{\partial \mathbf{a}(v_n)}{\partial v} \right\|_2} = \frac{j}{\|\mathbf{d}\|_2} \mathbf{d} \circ \exp\left(\frac{2\pi j}{\lambda} \cdot \frac{v_n}{v_P} \mathbf{d}\right).$$

Using $\hat{\mathbf{A}}$ we can reconstruct $\hat{\mathbf{x}}$ by (2), e.g. by the SPGl1-algorithm proposed in [7].

A first comparison of the quality of classical beamforming, original CS and the off-grid CS inspiried by a Taylor expansion is given in the simulative results in Figure 1. Here we use velocity grids $\mathcal{G}_v$ with $\delta_v = 1.2$ m/s on the left and 0.3 m/s on the right, both times ensuring $0 \in \mathcal{G}_v$. Furthermore, we define $\mathbf{d} = [-28.4, -9.6, 9.6, 28.4]$ cm, $v_P = 86$ m/s and $\lambda = 3$ cm. In both cases, we tried to reconstruct one target moving with a velocity that is in the middle between two gridpoints. In case of the off-grid CS we used the coefficients of the derivatives for repositionating the gridpoints. Clearly, the Taylor inspiried CS approach outperforms both, classical CS and beamforming in terms of leakage and positioning accuracy.

For real data computations we consider a data set with the same antenna parameters as for the simulations and use the grid $\{-3, -1.5, 0, 1.5, 3\}$ m/s. A SAR image of one channel is presented in Figure 2. For reasons of computation time we consider in the following just the area inside the red rectangle.

In the upper left corner of Figure 3, the reconstruction using CS without off-grid considerations – as proposed in Section II – is presented. This serves as a basis of comparison for the other results. The velocities and amplitudes of the moving targets are

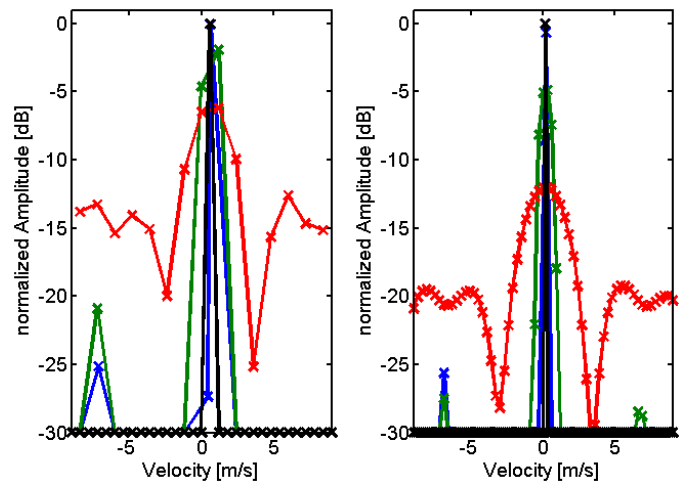

Figure 1. Reconstructions of one simulated signal at $v = 0.6$ m/s with $\delta_v = 1.2$ m/s (left) and at $v = 0.15$ m/s with $\delta_v = 0.3$ m/s (right), normalized to the same ℓ_2-norm using Taylor-CS (blue), classical CS (green) and beamforming (red) compared to the ground truth (black)

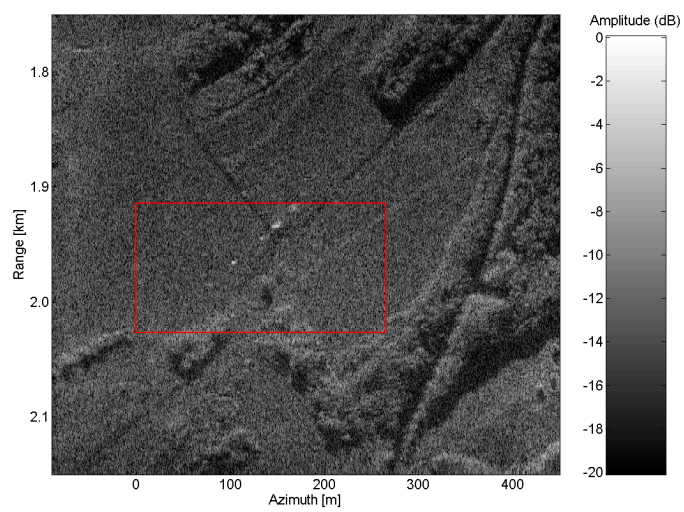

Figure 2. SAR image of one channel, area used for following figures is indicated by the red rectangle

depicted via the color defined by the colorbars in the lower right corner of Figure 3. For reasons of visibility we marked scatterers with velocity above 0.7 m/s and amplitude larger than 27 dB, only. In the upper right corner we see the result using the proposed aproach that considers off-grid velocities, while in the lower left corner this approach is expanded by jointly processing 4 neighbouring pixels and by using a weighted norm, enlarging probablility of the reconstruction of nonmoving targets. The latter is sensible, since moving targers are sparsely distributed in the whole scenery.

In all three images we see the 7 moving targets clearly reconstructed, while the remaining scenery is mostly filled with non moving clutter. The alarms above and beneath strong targets are induced by range sidelobes since range compression is performed using the classical matched filter. Consequently the only false alarm is that one in the upper right image at range 2086 m and azimuth 2150 m, being 1.4 dB above the threshold.

A much higher velocity resolution is the main advantage of the proposed approach. This is visible in Fig. 4. It presents sections at

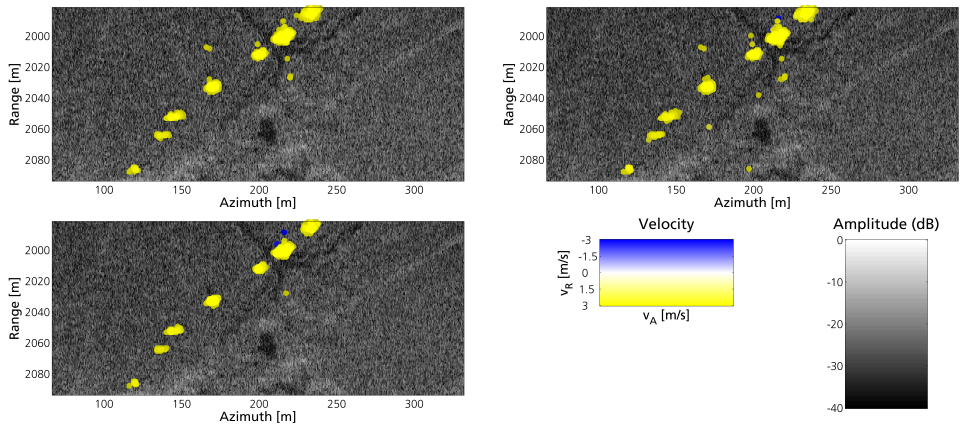

Figure 3. Reconstruction of the scenery marked in Fig. 2 using standard CS approach (without off-grid consideration, upper left), Taylor CS approach (upper right) and additional MMV and weighting (lower left)

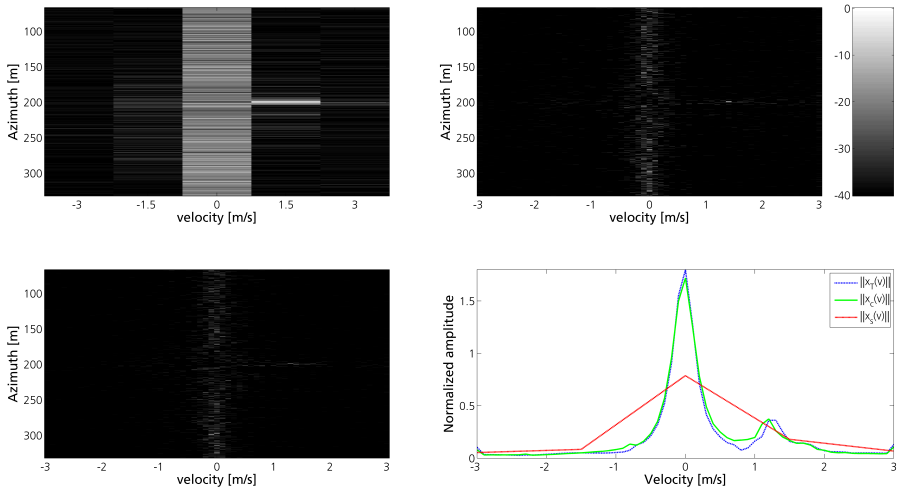

Figure 4. Sections through the results of Fig. 3 at range 2013 m and norms of the results of standard CS approach (x_s, upper left), Taylor based CS approach (x_T upper right) and polar interpolation based CS (x_c lower left) depending on the velocity

range 2013 m through the reconstructions without off-grid consideration (upper left), with off-grid consideration (upper right) on basis of the Taylor expansion and with off-grid consideration (lower left) on basis of the polar interpolation. In the upper left image, the clutter and the target (at 200 m in azimuth) are not separated and there is leakage of the target in other velocities. Both effects are reduced in case of off-grid CS, independent from the method, so the velocity can be determined better. Moreover, a variability of the clutter around 0 m/s can be observed, due to inner clutter movement.

At the lower left corner of Fig. 4 the plot of the norms of the same reconstructions, depending on the velocity, are presented. Since the targets move intentionally with approximately the same velocity, we see here a good separation between the clutter and the moving targets.

IV. Conclusion

In this paper we presented results of a new off-grid CS method to the problem of detecting ground moving targets from SAR images. Computations on simulated as well as on real data show its advantage over standard CS methods. This encourages further research regarding e.g. optimal parametrization or analysis of the approach's statistical behavior.

References

[1] R. G. Baraniuk, V. Cevher, M. F. Duarte, and C. Hegde. Model-based compressive sensing. *IEEE Transactions on Information Theory*, 56(4):1982–2001, Apr 2010.

[2] M. F. Duarte and R. G. Baraniuk. Spectral compressive sensing. *Applied and Computational Harmonic Analysis*, 35(1):111–129, Jul 2013.

[3] C. Ekanadham, D. Tranchina, and E. P. Simoncelli. Recovery of sparse translation-invariant signals with continuous basis pursuit. *IEEE Trans. on Signal Processing*, 59(10):4735–4744, Oct 2011.

[4] D. Cerutti-Maori and I. C. Sikaneta. A generalization of DPCA processing for multichannel SAR/GMTI radars. *IEEE Trans. on Geoscience and Remote Sensing*, 51(1):560–572, Jan 2013.

[5] L. Prünte. GMTI from multichannel SAR images using compressed sensing. In *Proceedings of the 9th European Conference on Syntetic Aperture Radar*, pages 199–202, Apr 2012.

[6] Y. C. Eldar and G. Kutyniok, editors. *Compressed Sensing: Theory and Applications*. Cambridge University Press, 1st edition, May 2012.

[7] E. van den Berg and M. P. Friedlander. Probing the Pareto frontier for basis pursuit solutions. *SIAM Journal on Scientific Computing*, 31(2):890–912, 2008.